JOURNAL OF APPLIED ELECTROCHEMISTRY **13** (1983) 307–315

High efficiency hypochlorite generation

P. M. ROBERTSON, W. GNEHM

Technisch Chemisches Labor, ETH, 8092 Zurich, Switzerland.

L. PONTO

Politechnika Warsaw, Poland.

Received 27 May 1982

The oxidation of chloride ion at DSA anodes gives higher yields of hypochlorite than were obtained at Pt or graphite electrodes. It is also shown that the problem of hypochlorite reduction at the cathode in undivided cells can largely be overcome by use of a 'reduced area' cathode. These two improvements have both been included in a new cylindrical hypochlorite cell capable of a 70% conversion of a $0.048\,\text{mol.dm}^{-3}$ NaCl solution to NaOCl with a production rate of $50\,\text{g}\,\text{h}^{-1}$ 'active chlorine'.

1. Introduction

Hypochlorite is found in widespread use for the disinfection of drinking water, sewage and process equipment in the food and beverage industries. It is also used to sterilize the cooling water of power stations to prevent fouling.

Because the transport of hypochlorite or more especially chlorine by road or rail is a serious environmental hazard, legislation is now being introduced in many countries which would in future prohibit the transport of these materials. The trend is therefore for on-site generation. Although the concentration of hypochlorite that can be reached by the direct electrolysis of chloride is not as high as that produced by the chemical method, it is sufficient for most purposes. Consumer demands, however, for better current efficiency or a higher degree of conversion of chloride to hypochlorite with less chlorate formation have led to several innovations in the field. We wish here to report some developments from our laboratories.

2. Chemistry of the process

The chemistry of the electro-oxidation of chloride has been well studied in the context of chlorate synthesis. It has recently been discussed in a comprehensive review article [1]. The main reactions are:

$$\text{Anode:}\qquad 2\text{Cl}^- \rightleftharpoons \text{Cl}_2 + 2\text{e} \tag{1}$$

$$6\text{OCl}^- + 3\text{H}_2\text{O} \rightleftharpoons 2\text{ClO}_3^- + 4\text{Cl}^- + 6\text{H}^+ + 3/2\text{O}_2 + 6\text{e} \tag{2}$$

$$2\text{H}_2\text{O} \rightleftharpoons \text{O}_2 + 4\text{H}^+ + 4\text{e} \tag{3}$$

$$\text{Cathode:}\qquad 2\text{H}_2\text{O} + 2\text{e} \rightleftharpoons \text{H}_2 + 2\text{OH}^- \tag{4}$$

$$\text{OCl}^- + \text{H}_2\text{O} + 2\text{e} \rightleftharpoons \text{Cl}^- + 2\text{OH}^- \tag{5}$$

$$\text{Solution bulk:}\ 2\text{HOCl} + \text{OCl}^- \rightleftharpoons \text{ClO}_3^- + 2\text{Cl}^- + 2\text{H}^+ \tag{6}$$

$$\text{Cl}_2 + \text{H}_2\text{O} \rightleftharpoons \text{ClO}^- + \text{Cl}^- + 2\text{H}^+ \tag{7}$$

where reactions 2, 5 and 6 in the case of hypochlorite production are the loss reactions. At low temperatures and outside of the pH range 4–6 the loss of active chlorine through the chemical formation of chlorate (Reaction 6) is negligible. The current efficiency and degree of conversion of chloride to hypochlorite is thereby limited by the extent of the side reactions 2, 3 and 5. The aim of this work was to find the optimal conditions for the minimization of these loss reactions (without recourse to additives such as chromate) and to apply the optimum conditions and operating parameters to a commercial hypochlorite generator. As will be shown here the improvement in performance that was obtained was considerable.

0021–891X/83 $03.00 + .12.

3. Investigation of the oxidation of chloride at a DSA anode [2]

3.1. *Apparatus*

Oxidations of chloride were carried out in batch experiments. The electrolyte was continuously pumped through a parallel plate cell (see Fig. 1). The electrode dimensions were 80 x 500 mm with an inter-electrode gap of 2 mm. The cathode was a titanium sheet and the anode a titanium sheet coated with ruthenium dioxide/ titanium dioxide. The coated anode (DSA) was prepared by the standard method of thermal oxidation of thin sprayed-on films of a solution of ruthenium and titanium trichlorides at about 400° C. Several layers were built-up by repeated treatment. The circulation path of the electrolyte consisted of three titanium tube heat exchangers which were connected to a cryostat, a reservoir with built-in baffles to enhance separation of gas and a ceramic centrifugal pump. Although the experiments were carried out in batch mode, the pH and NaCl concentration were kept constant by continuous addition of HCl and NaCl from Metrohm Dosimat motorised burettes. pH control was automatic and the Cl^- control semi-automatic, whereby the addition rate was initially set on the basis of the current and then corrected according to the measured Cl^- concentration.

The gas exiting from the circuit passed through a gas meter to measure the volumetric flow rate. The oxygen content of the gas stream was measured with an oxygen membrane electrode (Draeger Oxycom 25D). The concentrations of chloride, hypochlorite and chlorate were measured periodically during the course of an experiment until a well defined steady state was reached. Hypochlorite concentrations were measured by potentiometric titration using As_2O_3. At the end point for hypochlorite, the addition of OsO_4 catalyst and a low pH through the addition of H_2SO_4 allowed the determination of chlorate by further titration with As_2O_3. Thus the following parameters were known: volume of gas (V_{gas}), percentage of oxygen (X_{O_2}), current (I), and the concentrations, $c_{chloride}$, $c_{hypochlorite}$ and $c_{chlorate}$.

3.2. *Treatment of the results*

The rate of formation of hypochlorite, chlorate, hydrogen and oxygen were determined from the change of the appropriate measured parameter in the time interval between the measurements. The mass balance calculations followed through the application of the simplified scheme composed of the reactions: 1–5 and 7.

The loss reactions that have been neglected here, namely chemical chlorate formation, cathodic

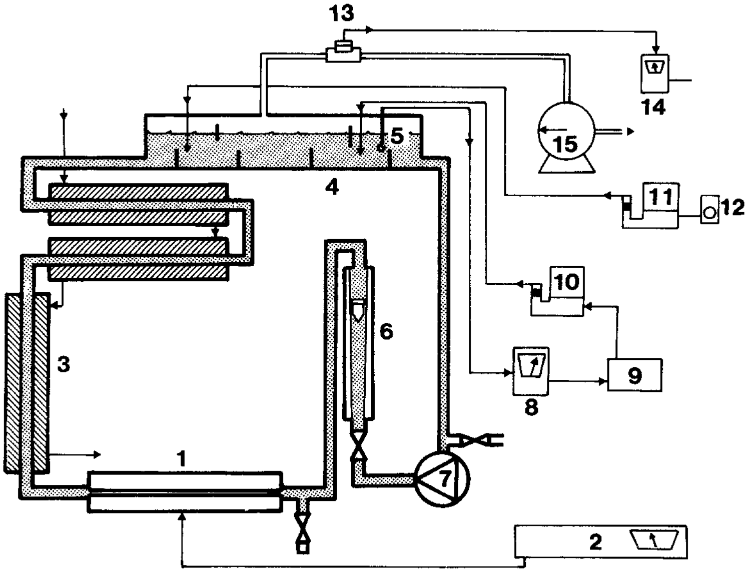

Fig. 1. Equipment for the study of the anodic oxidation of chloride. 1, electrolysis cell; 2, Sorensen power supply; 3, heat exchangers; 4, gas separator and reservoir; 5, pH-electrode; 6, flow meter; 7, centrifugal pump; 8, pH-meter; 9, Metrohm Impulsomat control; 10, 11, Metrohm Dosimat (motorized burette); 12, impulse generator; 13, O_2-meter and 14, control; 15, gas meter.

chlorate reduction, anodic perchlorate formation and loss of gaseous chlorine was justified on the basis of test experiments.

The current fractions for the formation or loss of the various species are given by:

$$t(\mathrm{OCl^-}) = 2F\,r(\mathrm{OCl^-})/60I$$

$$t(\mathrm{ClO_3^-}) = 6F\,r(\mathrm{ClO_3^-})/60I$$

$$t(\mathrm{O_{2\,F}}) = 3F\,r(\mathrm{ClO_3^-})/60I$$

$$t(\mathrm{H_2}) = 2F\,r(\mathrm{gas})(1 - X(\mathrm{O_2}))/60I$$

$$t(\mathrm{O_{2\,H_2O}}) = 2F\,r(\mathrm{gas})X(\mathrm{O_2})/60I - t(\mathrm{O_{2\,F}})$$

$$t(\mathrm{OCl_K^-}) = 1 - t(\mathrm{H_2})$$

where the current fraction $t(X)$ is that for the formation of the species X at rate $r(X)$. The subscripts F and H_2O refer to the contribution from the Foerster mechanism [2] and that due to water decomposition. The current fraction corresponding to the cathodic reduction of hypochlorite is given by $t(\mathrm{OCl_K^-})$.

A test of the material balance was given from the sum of the current fractions for the anodic reactions:

$$t_{\mathrm{anode}} = t(\mathrm{OCl^-}) + (\mathrm{OCl_K^-}) + t(\mathrm{ClO_3^-}) + t(\mathrm{O_{2\,F}}) + t(\mathrm{O_{2\,H_2O}})$$

3.3. *Results and discussion*

The results obtained during a batch electrolysis are given in Table 1. The concentration variations are shown in Fig. 2. After a time of 3–7 h (depending on the current density and the chloride concentration) a steady state hypochlorite concentration is reached. A summary of the steady state concentrations and production rates for 3 chloride concentrations two current densities and two flow rate is given in Table 2. These results have been calculated as described previously. Most experiments were performed at a nominal temperature of 10° C. For some runs at higher current densities the cooling was inadequate and the temperature rose slightly. The pH was controlled to within 0.05 units.

The stationary hypochlorite concentration was found to be very sensitive to the current density and electrolyte flow velocity. A doubling of the current density resulted in about a 70% increase in the steady state hypochlorite concentration, whereas a 50% increase in the electrolyte velocity gave a 60% drop. The reason for such behaviour is probably that the chloride oxidation to hypochlorite is taking place somewhat under the limiting current (steady state concentration dependence on I) and a diffusion controlled cathodic loss reaction occurs.

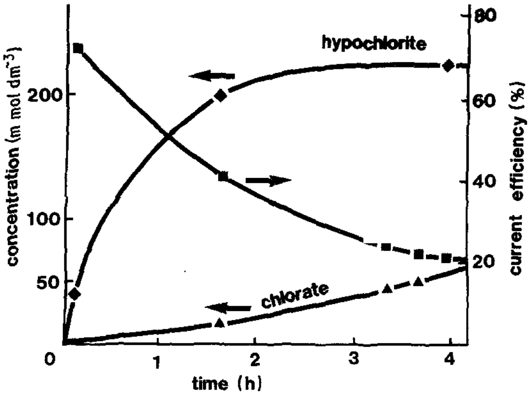

Fig. 2. Concentrations of hypochlorite and chlorate and the current efficiency for hypochlorite formation during a batch electrolysis with the following experimental conditions. $c_{\mathrm{Cl^-}}$, 0.46 mol dm^{-3}; temperature, 10.8° C; pH, 8.5, flow velocity 65 cm s^{-1} and i, 200 mA cm^{-2}.

The production rate data in Table 2 has also been expressed as a pseudo mass transfer coefficient defined as:

$$r_{\mathrm{prod}}/Ac_{\mathrm{feed}}\ (\mathrm{cm\,s^{-1}}).$$

where A is the electrode area. These pseudo mass transfer coefficients are given in Figs. 3 and 4 as a function of the electrolyte flow velocity. They show that the reduction of hypochlorite to chloride correlates with the electrolyte velocity, whereas the rates for the oxidation of hypochlorite to chlorate shows no correlation with electrolyte flow velocity. The latter result is in contrast with those of Ibl and Landolt (3–5) for chloride oxidation with platinum and graphite electrodes.

Thus at DSA anodes based on RuO_2 and at the current densities employed here the further oxidation of hypochlorite is kinetically controlled. Estimates of the fluxes of chloride and hypochlorite to the anode showed that the value for chloride lay closer to the limiting one than that for hypochlorite. Thus at DSA anodes the anodic loss of hypochlorite proceeds at a lower rate than at platinized titanium and allows not only a higher

Table 1. Results of batch electrolysis

Time (min)	c_{Cl^-} (mmol dm^{-3})	c_{ClO_3} (mmol dm^{-3})	V_{gas} dm^3	$X(\mathrm{O}_2)$	r_{OCl^-} (mmol dm^{-3} min^{-1})	$r_{\mathrm{ClO}_3^-}$ (mmol dm^{-3} min^{-1})	r_{gas} (mmol dm^{-3} min^{-1})	r_{O_2} (mmol dm^{-3} min^{-1})	$c^{\mathrm{c}}_{\mathrm{OCl}^-}$ (mmol dm^{-3} min^{-1})
0	0.0	0.0	0.00						
10	0.036	0.011	5.42	0.10	14.3	0.438	21.4	12.14	1.0
100	0.201	0.0168	33.60	0.08	7.5	0.708	12.3	0.99	8.9
200	0.226	0.0433	56.33	0.15	1.2	1.097	9.0	1.33	12.6
220	0.227	0.0498	60.82	0.16	0.5	1.380	8.9	1.43	12.7
240	0.228	0.0570	65.27	0.16	0.3	1.471	8.8	1.42	12.8

V_{gas}: gas volume.
r_{gas}: total rate of gas production.
r_{O_2}: rate of oxygen production.
$c^{\mathrm{c}}_{\mathrm{OCl}^-}$: rate of reduction of hypochlorite at the cathode.

Table 2. A summary of steady state concentrations and production rates

Number	c_{Cl^-} (mmol dm^{-3})	T (°C)	pH	u (cm s^{-1})	i (mA cm^{-2})	E (V)	c_{OCl^-}(st) mol dm^{-3}	$r_{\mathrm{OCl}_3^-}$ (mmol dm^{-3} min^{-1})	$r_{\mathrm{ClO}_3^-}$ (mmol dm^{-3} min^{-1})	$r^{\mathrm{c}}_{\mathrm{ClO}^-}$ (mmol dm^{-3} min^{-1})	r_{gas} (mmol dm^{-3} min^{-1})	r_{O_2} (mmol dm^{-3} min^{-1})	$10^3 k^*_{\mathrm{OCl}^-}$ cm s^{-1}	$10^3 k^*_{\mathrm{ClO}_3^-}$ cm s^{-1}
11	0.070	6.5	8.5	52	40	5.1	0.060	0.35	0.188	2.39	2.04	0.39	2.04	4.82
12	0.074	9.0	8.5	91	40	5.0	0.044	0.06	0.094	3.03	1.30	0.28	3.53	3.29
13a	0.054	10.0	8.5	66	20	4.2	1.029	0.00	0.053	1.61	0.54	0.13	2.85	2.81
13b	0.059	10.0	8.5	100	20	3.9	0.022	< 0	0.042	–	–	–	–	–
14a	0.49	10.0	8.5	90	40	3.4	0.052	0.17	0.043	3.67	0.47	0.12	3.62	1.27
14b	0.48	10.0	8.5	65	40	3.5	0.069	0.10	0.118	3.48	0.70	0.13	2.59	2.63
10	0.62	17.0	8.5	89	200	4.8	0.151	0.92	0.548	15.10	6.07	0.97	5.13	5.58
17	0.46	10.8	8.5	65	200	5.4	0.228	0.38	1.43	12.78	8.86	1.43	2.87	9.65
9	0.56	9.8	8.5	51	200	5.0	0.243	0.93	1.6	11.73	9.95	1.46	2.48	10.13
15a	3.5	9.9	8.5	81	40	3.1	0.083	0.15	0.046	3.56	0.58	0.09	2.20	0.85
15b	3.4	9.9	8.5	59	40	3.1	0.106	0.12	0.094	3.30	0.86	0.12	1.60	1.36
16a	3.5	13.0	8.5	80	200	4.0	0.277	0.48	1.54	13.01	8.36	1.06	2.41	8.55
16b	3.4	10.0	8.5	57	200	4.1	0.368	0.74	1.67	11.68	9.86	1.32	1.63	6.98
8	0.45	12.0	8.5	75	200	7.2	0.291	0.60	3.60	2.1	12.6	3.5	0.37	19.03

c_{Cl^-}: average chloride concentration in steady state.
u: linear electrolyte velocity.
i: current density.
E: cell voltage.
c_{OCl^-}(st): hypochlorite concentration in stationary state.
r_{OCl^-}: effective rate of formation of hypochlorite.
$c^{\mathrm{c}}_{\mathrm{OCl}^-}$: rate of reduction of hypochlorite at the cathode.
r_{gas}: total rate of gas production.
r_{O_2}: rate of oxygen production.
$k^*_{\mathrm{OCl}^-}$: pseudo mass transfer rate of hypochlorite to the cathode.
$k^*_{\mathrm{ClO}_3^-}$: pseudo mass transfer rate of hypochlorite to the anode.

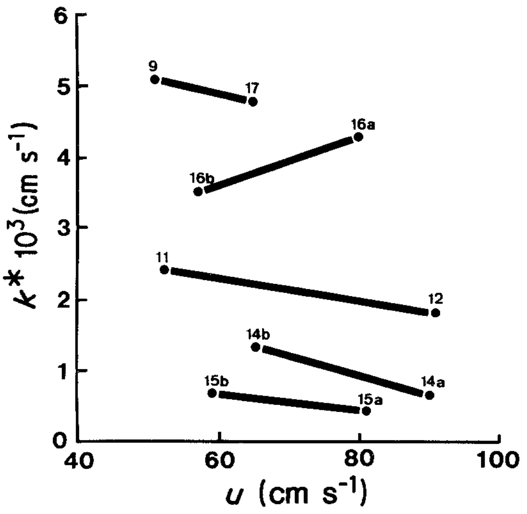

Fig. 3. Pseudo mass transfer coefficients as a function of electrolyte flow rate, hypochlorite to anode.

current efficiency for hypochlorite to be attained but also a higher degree of conversion. This was also verified in experiments with Ti/Pt and Ti/RuO$_2$ electrodes but otherwise identical conditions. The results of these experiments have also been expressed in terms of the individual current efficiencies for O$_2$ evolution, hypochlorite formation, chlorate formation and cathodic hypochlorite reduction as a function of the concentration of available chlorine. Some of these results are given in Fig. 5. From the outset of our studies it was clear that the cathodic loss of hypochlorite was a reaction that had to be hindered if a higher performance hypochlorite generator was to be constructed. The use of a porous plastic covering on the counter electrode to dampen convection and thereby lower the mass transfer coefficient has been investigated (6, 7). In this work specially prepared cathodes with reduced active electrode areas were employed. The cathodes used in the parallel plate cell were constructed by milling 'V'-grooves along the x and y coordinates of the cathode surface so as to form pyramids of base area 2 mm, mounting the electrode in Araldite and filing the excess Araldite down until the points of the pyramids were exposed. (The reduced area electrode constructions are described in a recently filed Swiss Patent Application.) The results obtained with such an electrode (the exact surface area of which was unknown but probably less than 1% of the plate area) are shown in Fig. 5c. As shown the cathodic loss reaction was almost completely eliminated.

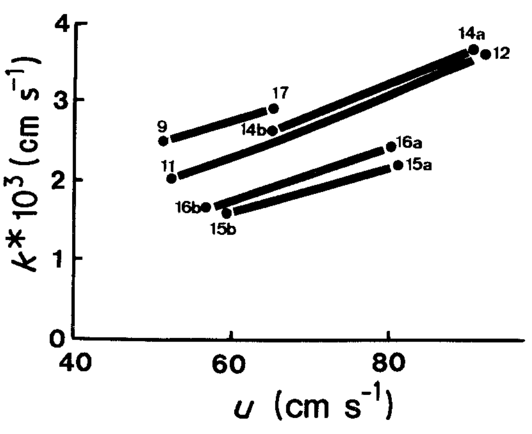

Fig. 4. Pseudo mass transfer coefficients as a function of electrolyte flow rate, hypochlorite to cathode.

The practical significance of our results can be summarized as follows:

DSA anodes give superior results to platinized titanium; highest conversions to hypochlorite are obtained at low chloride concentrations (Fig. 5a) and with a special reduced area cathode to which a minimal flux of hypochlorite flows (Fig. 5c).

4. Optimization of a commercial hypochlorite generator

4.1. *Description of the equipment*

The commercial hypochlorite generator was a compact unit with a nominal capacity of 50 g 'active chlorine' per hour. The electrolysis cell was a concentric construction, 50 cm in length and 5 cm diameter. The outer titanium tube was platinized on the inside surface and acted as the anode. A 24 mm diameter graphite rod was used as a cathode. The inter-electrode gap was 12 mm.

Electrolyte was prepared by continuously injecting a saturated NaCl solution with a membrane pump into a steady flow of tap water which then passed through the cell. This solution was electrolysed in a single pass. A schematic diagram of the equipment is given in Fig. 6.

The unit on which our optimized conditions were put into practise had a capacity of up to 500 g 'active chlorine' per hour.

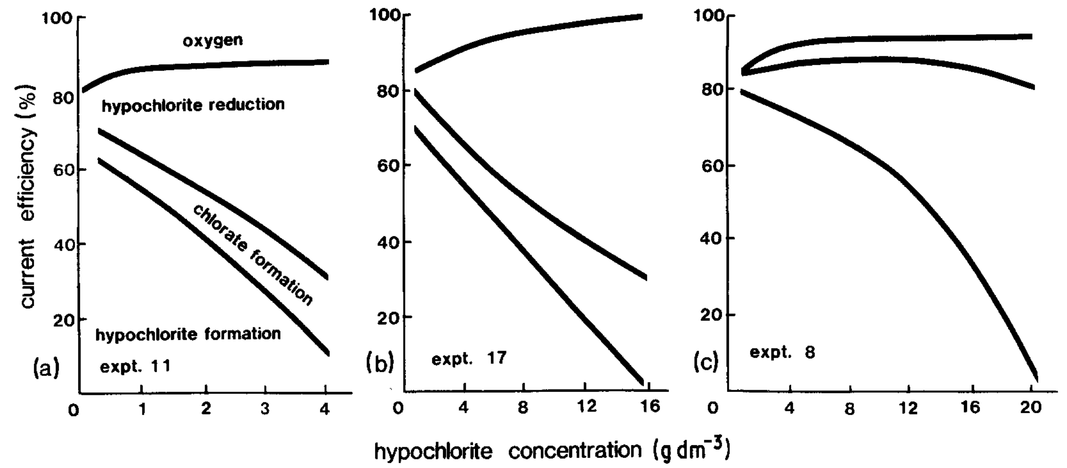

Fig. 5. Individual components making up the overall current efficiency. See Table 2 for experimental conditions.

4.2. *Goal of the optimization*

The goal of the optimization was to maximize the conversion of NaCl to hypochlorite. This is especially important in swimming pool applications where a certain hypochlorite concentration is required but at the lowest possible salt concentration.

Several constraints had also to be observed:

production capacity not less than 50 g h^{-1}
maximum operating temperature of 50° C.

On the basis of the aforementioned results with DSA electrodes this goal might be reached by the use of low NaCl concentrations and a special cathode with reduced area.

4.3. *Results*

Preliminary experiments with the original cell equipped with a platinized titanium anode over a range of flow rates showed that the required performance of 50 g h^{-1} 'active chlorine' could not be realized. In fact values of about 20 g h^{-1} were not exceeded. The cell was therefore rebuilt with a DSA anode. This was prepared as described in Section 3.1. Later commercial electrolysers incorporated DSA anodes of the Permelec company in Milan. These had a coating formulation that was best suited for operation at low chloride concentrations. At the same time the cathode diameter was increased to 40 mm thereby reducing the inter-electrode gap to 4 mm and more important a reduced area construction was employed. This was constructed by mounting a graphite rod, onto which a spiral thread had been cut, in Araldite and then removing the excess Araldite on a lathe until the tops of the thread were exposed. It was anticipated that the smaller inter-electrode gap would allow higher current densities (and a higher degree of conversion) while not exceedings the 50° C maximum

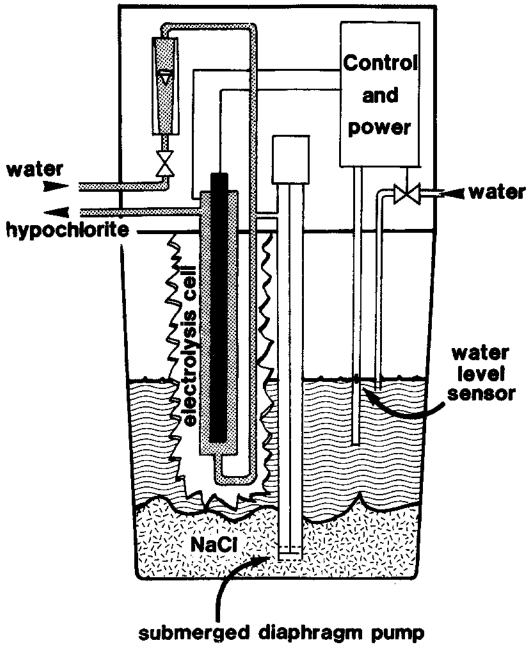

Fig. 6. Schematic diagram of commercial electrolysis system for the generation of hypochlorite.

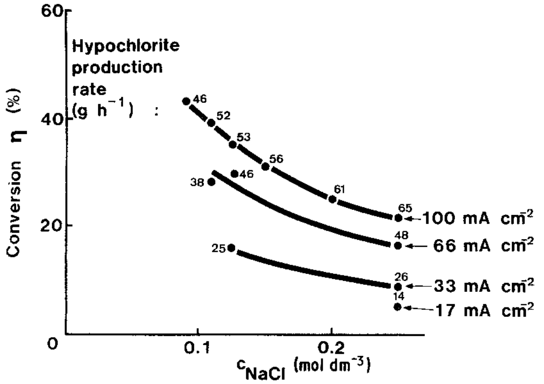

Fig. 7. Performance of a 50 cm long hypochlorite cell with a DSA anode.

allowed operating temperature. The results of some optimization experiments with the modified cell are given in Fig. 7. In these experiments current density, electrolyte flow rate and c_{NaCl} were varied. At the flow rate of 0.27 $\mathrm{dm^{-3}\ min^{-1}}$ (0.81 $\mathrm{cm\ s^{-1}}$) used in these runs, the highest conversion of chloride to hypochlorite was achieved using the highest current density (100 $\mathrm{mA\ cm^{-2}}$) and lowest c_{NaCl} (0.09 mol $\mathrm{dm^{-3}}$ for which $\eta = 43\%$. With the DSA anode there was no problem in reaching the required 50 $\mathrm{g\ h^{-1}}$ hypochlorite production rate.

It was interesting to compare the performance of the cell with DSA anode to the original cell with a platinized titanium anode. Two experiments with the two cells were carried out using identical electrolysis conditions (100 mA $\mathrm{cm^{-2}}$, 0.27 $\mathrm{dm^{-3}\ min^{-1}}$, 0.09 mol $\mathrm{dm^{-3}}$ NaCl). The results are given in Table 3.

Apparently the DSA anode allows the oxidation of chloride with a much higher current efficiency and gives an insignificant amount of chlorate in comparison to the platinum anode.

Although a considerable improvement had already been achieved it was thought that the limited residence time of the electrolyte in the cell restricted the conversion below that theoretically realizable with the electrode configuration employed.

Table 3. A comparison of DSA and Ti/Pt anodes

	$c_{\mathrm{ClO^-}}$ ($\mathrm{mol\,dm^{-3}}$)	$c_{\mathrm{ClO_3^-}}$ ($\mathrm{mol\,dm^{-3}}$)
DSA	0.0385	0.0016
Ti/Pt	0.0197	0.009

A 1 m long cell with tap-off points every 10 cm allowed measurement of the conversion as a function of electrode length. The results for the oxidation of chloride, which confirmed our expectations, are shown in Fig. 8. These experiments were carried out at lower NaCl concentrations for which a smaller inter-electrode gap was required on account of the potential drop and heat production. The results shown in Fig. 8 were obtained with cells having inter-electrode gaps of 2, 3 and 5 mm. Here the full 1 m reactor length was employed. The results are plotted against the production rate reached for several values of the current density, electrolyte flow velocity and chloride concentration. For the experiments run at the low NaCl concentration of 0.048 mol $\mathrm{dm^{-3}}$ (series c, d and e) a conversion of over 70% could be achieved while still giving a production rate of hypochlorite of 50 $\mathrm{g\,h^{-1}}$ or more. Another set of data obtained with the 100 cm cell is shown in Fig. 9. Here the conversion is plotted as a function of the current density. These results show that the *in situ* electrolytic production of hypochlorite (when carried out under optimal conditions) gives a superior product with a higher $c_{\mathrm{OCl^-}}/c_{\mathrm{Cl^-}}$ ratio (~ 4) than is possible using a chlorine gas treatment, where the hydrolysis of chlorine automatically leads to a concentration ratio in the product stream of 1:

$$\mathrm{Cl_2 + H_2O \rightleftharpoons OCl^- + Cl^- + 2H^+}$$

Measurement of the hypochlorite concencentration as a function of the reactor length showed that the highest conversions were already attained with a reactor length of 60–70 cm (Fig. 10). The minimum length of the reactor for the maximum conversion to be achieved was found to be dependent on the magnitude of the inter-electrode gap. Smaller gaps gave shorter lengths for attaining the limiting conversion, for example 65 cm with a 2 mm gap and 90 cm with a 5 mm gap.

The optimum conditions that we have determined here are now being employed in the current hypochlorite generators of the company Korthals AG, Ruschlikon, Switzerland. They result in about a x 4 improvement (degree of conversion, production rate) over the generator employing platinized titanium anodes.

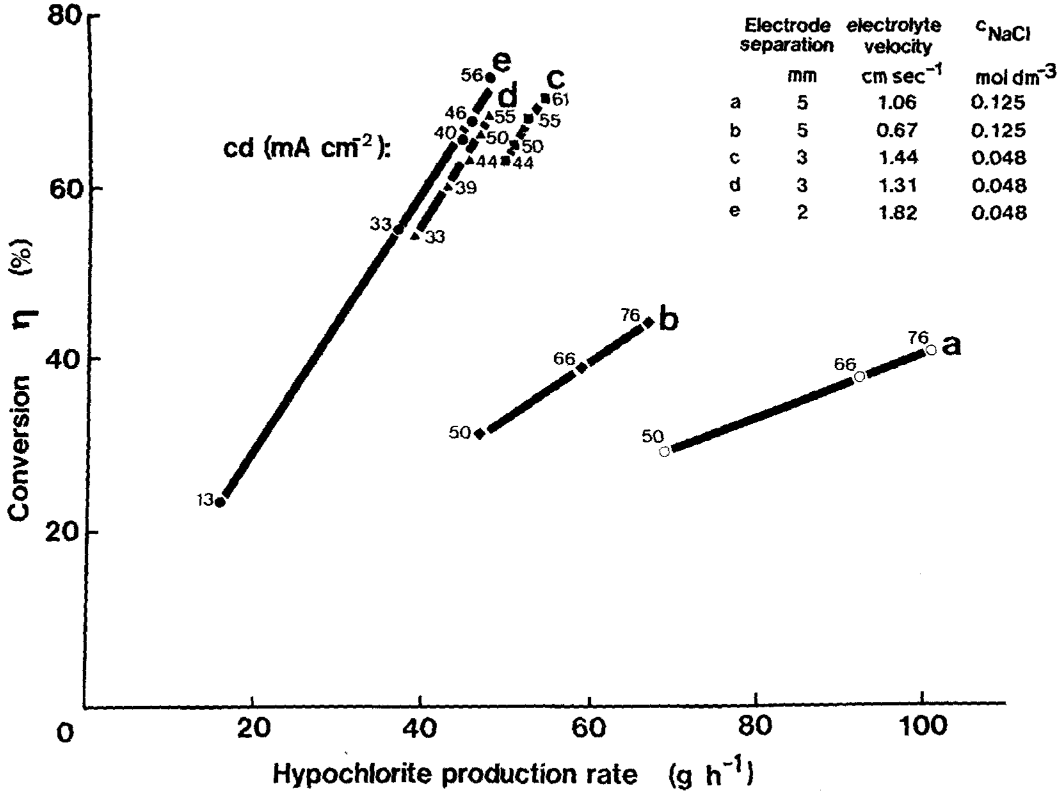

	Electrode separation	electrolyte velocity	c_{NaCl}
	mm	cm sec^{-1}	mol dm^{-3}
a	5	1.06	0.125
b	5	0.67	0.125
c	3	1.44	0.048
d	3	1.31	0.048
e	2	1.82	0.048

Fig. 8. Performance of a 100 cm long hypochlorite cell with a DSA anode.

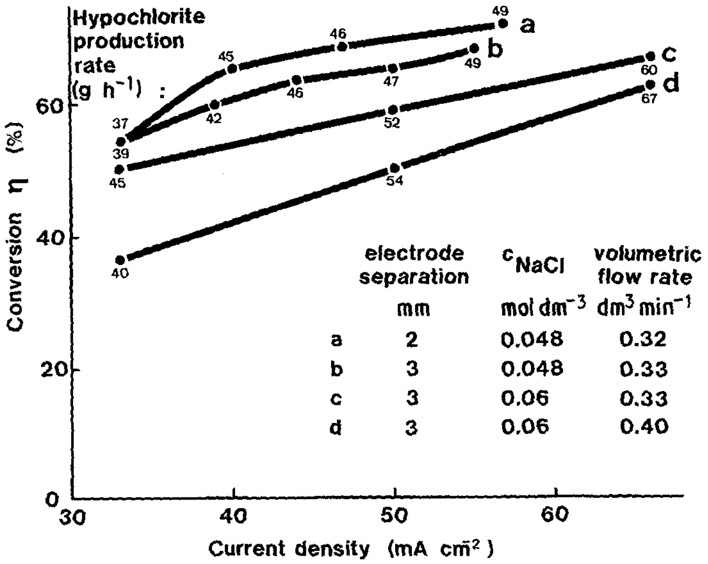

	electrode separation	c_{NaCl}	volumetric flow rate
	mm	mol dm^{-3}	dm^3 min^{-1}
a	2	0.048	0.32
b	3	0.048	0.33
c	3	0.06	0.33
d	3	0.06	0.40

Fig. 9. Performance of a 100 cm long hypochlorite cell with a DSA anode.

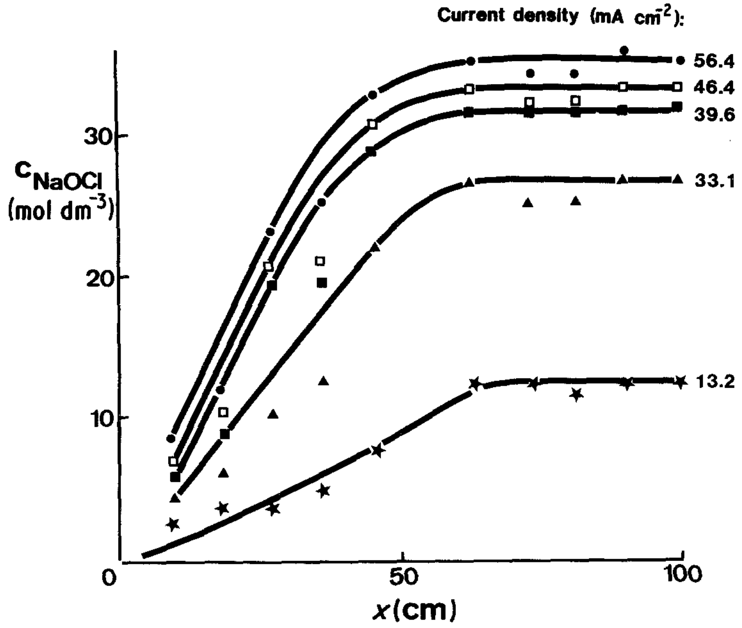

Fig. 10. Electrolysis of 48 mmol dm^{-3} NaCl with various reactor lengths.

5. Conclusions

A study of the anodic oxidation of chloride at DSA anodes showed that considerably higher yields of hypochlorite were obtained than at platinum or graphite anodes. Further, the oxidation of hypochlorite to chlorate was found to be mass transfer controlled (as at platinum or graphite electrodes) and allowed therefore a much higher conversion of chloride to hypochlorite to be achieved. The conditions for maximizing this conversion were low chloride concentration and high current density. A parametric study and optimization of a commercial hypochlorite generator on the basis of the aforementioned trends resulted in a greatly improved performance.

6. Acknowledgement

We are grateful for the financial support of this work by Korthals AG, Rueschlikon, Switzerland.

References

[1] N. Ibl and H. Vogt, in 'Comprehensive Treatise on Electrochemistry', Vol. 2, (edited by J. O'M. Bockris, B. E. Conway, E. Yeager and R. E. White) Plenum Press, New York, (1981).
[2] W. Gnehm, ETH Diplomarbeit, TCL number 3983, (1981).
[3] N. Ibl and D. Landolt, *J. Electrochem. Soc.* **115** (1978) 713.
[4] D. Landolt and N. Ibl, *Electrochim. Acta* **15** (1970) 1165.
[5] *Idem*, *J. Appl. Electrochem.* 2 (1972) 201.
[6] D. Matic, P. M. Robertson and N. Ibl, *Electrochim. Acta* **25** (1980) 478.
[7] P. M. Robertson, R. Oberlin and N. Ibl, *Electrochim. Acta* **26** (1981) 941.